

# The radial alignment of dark matter subhalos: from simulations to observations

Alexander Knebe<sup>1</sup>, Hideki Yahagi<sup>2,3,4,5,6</sup>, Hiroyuki Kase<sup>2,7</sup>, Geraint Lewis<sup>8</sup>,  
Brad K. Gibson<sup>5,8</sup>

<sup>1</sup>*Astrophysikalisches Institut Potsdam, An der Sternwarte 16, Germany*

<sup>2</sup>*Department of Astronomy, University of Tokyo, Tokyo 113-0033, Japan*

<sup>3</sup>*Division of Theoretical Astronomy, National Astronomical Observatory, Japan*

<sup>4</sup>*Research Fellow of the Japan Society for the Promotion of Science*

<sup>5</sup>*Centre for Astrophysics, University of Central Lancashire, Preston PR1 2HE, UK*

<sup>6</sup>*Research Institute for Information Technology, University of Kyushu, Fukuoka 812-8581, Japan*

<sup>7</sup>*present address: Prometech Inc., 7-3-1 Hongo, Bunkyo, Tokyo 113-0033, Japan*

<sup>8</sup>*School of Physics, University of Sydney, Sydney NSW 2006, Australia*

Submitted Version ...

## ABSTRACT

We explore the radial alignment of subhalos in 2-dimensional projections of cosmological simulations. While most other recent studies focussed on quantifying the signal utilizing the full 3-dimensional spatial information any comparison to observational data has to be done in projection along random lines-of-sight. We have a suite of well resolved host dark matter halos at our disposal ranging from  $6 \times 10^{14} h^{-1} M_{\odot}$  down to  $6 \times 10^{13} h^{-1} M_{\odot}$ . For these host systems we do observe that the major axis of the projected 2D mass distribution of subhalos aligns with its (projected) distance vector to the host’s centre. The signal is actually stronger than the observed alignment. However, when considering only the innermost 10-20% of the subhalo’s particles for the 2D shape measurement we recover the observed correlation. We further acknowledge that this signal is independent of subhalo mass.

**Key words:** galaxies: evolution – galaxies: halos – cosmology: theory – cosmology: dark matter – methods:  $N$ -body simulations

## 1 INTRODUCTION

The concordance of a multitude of recent cosmological studies has demonstrated that we appear to live in a spatially flat,  $\Lambda$ -dominated cold dark matter ( $\Lambda$ CDM) universe (cf. Spergel et al. 2007). During the past decade simulation codes and computer hardware have advanced to such a stage where it has been possible to resolve in detail the formation of dark matter halos and their subhalo populations in a cosmological context (e.g. Klypin et al. 1999). These results, coupled with the simultaneous increase in observational data (e.g. 2 degree Field galaxy redshift survey (2dFGRS), Colless (2003); Sloan Digital Sky Survey (SDSS), Adelman-McCarthy (2007)), have opened up a whole new window on the concordance cosmogony in the field that has become known as “near-field cosmology” (Freeman & Bland-Hawthorn 2002).

One particular property of the satellite population that has caught the attention of simulators recently is the radial alignment of their primary axes of subhalos with respect to the distance vector to the host’s centre. The first evidence

for this effect was reported for the Coma cluster, where it was observed that the projected major axes of cluster members preferentially align with the direction to the cluster centre (Hawley & Peebles 1975; Thompson 1976). Such a correlation between satellite elongation and radius vector has further been confirmed by statistical analysis of the SDSS data (Pereira & Kuhn 2005; Agustsson & Brainerd 2006; Faltenbacher et al. 2007; Wang et al. 2007). The radial alignment of subhalo shapes towards the centre of their host has also been measured for the subhalo population in cosmological simulations (Knebe et al. 2008; Kuhlen et al. 2007; Faltenbacher et al. 2007; Pereira et al. 2007). We though note that all these authors used the 3-dimensional spatial information available to them. However, any fair comparison to the signal found observationally requires the projection of the simulation data into an observer’s plane, i.e. averaging over a substantial number of 2D restrictions of the data (cf. Faltenbacher et al. 2007). This is the primary motivation for the present study: *Can we still find a*

signal of radial alignment when limiting the simulation data to 2D?

In this *Letter* we provide evidence that the radial alignment of subhalos in cosmological simulations – when projected into two dimensions – is substantially stronger than found in observations. We though recover the observed correlation strength when restricting the shape measurement to the innermost 10-20% of the subhalos’ particles; this result supports the findings of Faltenbacher et al. (2007) who also used the inner regions of their satellite halos as a proxy for the orientation of a hypothetical galaxy and found good agreement with the measurements from SDSS data. We further show that the signal does not depend on the mass of the actual subhalo.

## 2 METHOD

### 2.1 Simulations

The cosmological  $N$ -body simulation employed in this study was generated as part of the Numerical Galaxy Catalog program (Nagashima et al. 2005). Utilizing a parallel version of an established  $N$ -body code (Yahagi & Yoshii 2001; Yahagi 2005), the algorithm uses an adaptive mesh refinement technique to maintain accuracy (cf. Kravtsov et al. 1997; Knebe et al. 2001; Yahagi & Yoshii 2001; Teyssier 2002). The simulation considered a region of the universe with a boxsize of  $70 h^{-1}$  Mpc (comoving), with  $512^3$  particles, resulting in a particle mass of  $3.04 \times 10^8 h^{-1} M_\odot$ . The adopted cosmological parameters represent a concordance  $\Lambda$ CDM model with  $\Omega_m = 0.3$ ,  $\Omega_\Lambda = 0.7$ ,  $h = 0.7$ , and  $\sigma_8 = 0.9$  (cf. Spergel et al. 2003). The simulation was started at  $z = 41$  and analysed at  $z = 0$ .

### 2.2 (Sub-)Halo Identification

In extracting groups and subhalos, the standard friends-of-friends (FoF) method was employed (Davis et al. 1985), with the ratio of the linking length to the mean separation of particles  $b = 0.2$ , and cluster and group scale host halos were chosen to have masses in the range,  $6.45 \times 10^{13} h^{-1} M_\odot \leq M_{\text{host}} \leq 5.95 \times 10^{14} h^{-1} M_\odot$ . Once these host halos were identified, a hierarchical finder based on the FoF (HFoF) method (Klypin et al. 1999) used to isolate subhalos, employing successively decreasing linking length. Furthermore, the evaporative method was used to discard unbound subhalos (Pfitzer et al. 1997), and all unbound particles were removed from the subhalos. At this stage, we calculated potential energy of particles in subhalos iteratively, defining a minimum subhalo as containing 100 particles.<sup>1</sup> While this is very time consuming procedure, the process was accelerated by employing a special purpose computer for self-gravitating system, GRAPE-6 (Makino et al. 2003); details of the subhalo finding are given in Kase et al. (2007).

<sup>1</sup> We note that this is a conservative criterion as other studies indicate that halo catalogues are complete for objects containing in excess of  $\geq 50$  particles (e.g. Kravtsov et al. 2004; Allgood et al. 2006).

**Table 1.** Number of subhalos in a certain mass range.

$M$	$N_{\text{sub}}$
$M < 10^{11} h^{-1} M_\odot$	1199
$M \in [10^{11}, 10^{12}] h^{-1} M_\odot$	846
$M \in [10^{12}, 10^{13}] h^{-1} M_\odot$	120
$M \in [10^{13}, 10^{14}] h^{-1} M_\odot$	23

We ended up with 40 host halos with a combined number of 2188 subhalos in excess of 100 particles. In the following analysis we stack the information from all these hosts and present the results in one single plot. We are confident not to obscure any signal as it has recently been shown that the radial alignment is independent on the host mass (Knebe et al. 2008).

When investigating the dependence of radial alignment on the mass of the subhalos we split the subhalos into three mass bins, i.e.  $[10^{11}, 10^{12}] h^{-1} M_\odot$ ,  $[10^{12}, 10^{13}] h^{-1} M_\odot$ , and  $[10^{13}, 10^{14}] h^{-1} M_\odot$ . The total number of subhalos in each of these bins (as well as the number of subhalos with  $M < 10^{11} h^{-1} M_\odot$  is given in Table 1. We further like to note that the most massive subhalo weights  $M_{\text{sub}}^{\text{max}} = 2.9 \times 10^{13} h^{-1} M_\odot$  and belongs to a  $M_{\text{host}} = 1.6 \times 10^{14} h^{-1} M_\odot$  host halo.

## 3 RESULTS

Our view of clusters of galaxies upon the sky is a projection of the true, three dimensional distribution and orientation of halos and their associated galaxies. In this study, we therefore consider projected views of our simulated halos, adopting 19 projections in both azimuthal angle and cosine of latitudinal angle, respectively. The results presented subsequently in this study average over these differing orientations.

### 3.1 Subhalo Shapes in 2D

The principal axes of the projected two-dimensional density distributions of all our subhalos were calculated using the reduced moment of inertia tensor (Katz 1991; Dubinski & Carlberg 1991)<sup>2</sup>,

$$\hat{I}_{i,j} = \frac{1}{N_p} \sum_{l=1}^{N_p} \frac{x_{l,i} x_{l,j}}{\zeta_l^2}, \quad (1)$$

$$\zeta_l^2 = x_l^2 + \left(\frac{y_l}{s}\right)^2, \quad (2)$$

where  $x_{l,i}$  is  $i$ -th component of projected (2-dimensional) position of the  $l$ -th constituent particle, and  $N_p$  is the number of particles in the subhalo. Solving for the eigensystem of this tensor identifies the principle axes of the distribution. We then define the sphericity

$$s = \frac{a_2}{a_1} \quad (3)$$

<sup>2</sup> We like to note in passing that it makes little difference using either the reduced or the "standard" moment of inertia tensor that does not include the  $1/\zeta_l^2$  term.

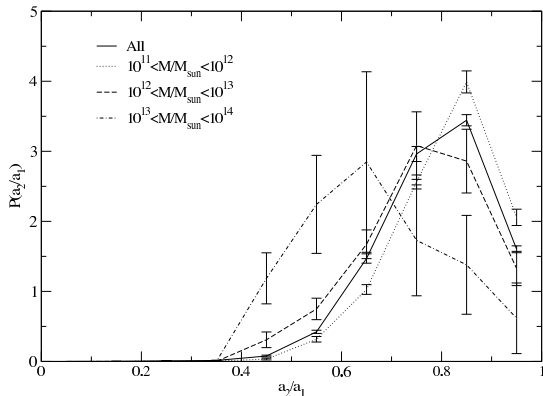


**Figure 1.** Distribution of the 2D sphericity  $s = a_2/a_1$ . Solid line indicates the distribution of axis ratio using all subhalos. The different lines represent restrictions of the subhalo masses under consideration to the intervals  $[10^{11}, 10^{12}]h^{-1}M_\odot$ ,  $[10^{12}, 10^{13}]h^{-1}M_\odot$ , and  $[10^{13}, 10^{14}]h^{-1}M_\odot$ . Error bars indicate the square root of the sum of the Poisson error and the projection variation.

of a (projected) subhalo as the ratio of the minor to major axis. The procedure in determining these principle axes has to be done iteratively, starting with the assumption of sphericity  $s = 1$ . The eigensystem is solved for  $s$  until the value converges.

### 3.1.1 Mass Dependence

In Fig.1 we examine the variation of the (normalized) probability distribution  $P(s = a_2/a_1)$  of sphericity with subhalo mass. We observe a (marginal) trend for  $s$  to decrease with increasing subhalo mass – as reported by Allgood et al. (2006) for field halos. We also note that the projected sphericities are of similar value to the 3D sphericities as found in Knebe et al. (2008) making a study of radial alignment feasible. We need to stress that the number statistics for the subhalo mass bin  $[10^{13}, 10^{14}]h^{-1}M_\odot$  is rather small (cf. Table 1); there are a mere 23 subhalos in the respective mass range and hence the large error bars. As these objects are in fact rather massive and comparable to the actual host halos, we are not surprised to find sphericities closer to those of isolated/field halos ( $\langle s \rangle \approx 0.66$ , cf. Frenk et al. 1988; Warren et al. 1992; Kasun & Evrard 2005; Bailin & Steinmetz 2005; Allgood et al. 2006; Macciò et al. 2007; Bett et al. 2007)

### 3.1.2 Radial Dependence

As with many cosmological  $N$ -body studies, we are considering the orientations of *dark matter* (sub-)halos and are comparing them with the distributions of *baryons* observed in galaxy clusters. Such a comparison can be significantly biased if the observed orientation of galaxies, which occupy the deepest part of the subhalo potential, are not aligned with the global orientation of the dark matter (cf. Bailin & Steinmetz 2005). Hence we also present the variation of subhalo sphericity (as well as the radial alignment in Section 3.2.2) with distance to its centre.

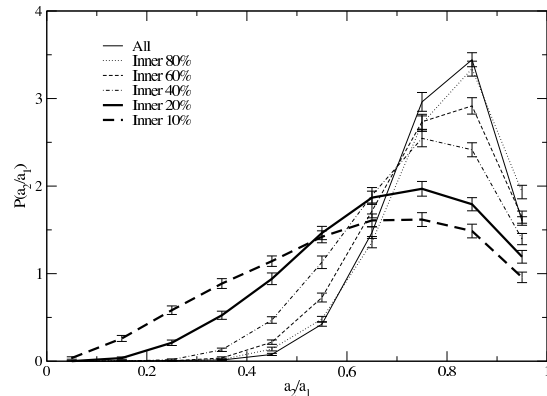


**Figure 2.** Distribution of the 2D sphericity  $s = a_2/a_1$ . The different lines represent shape measures at different mass thresholds. Error bars indicate the projection variation.

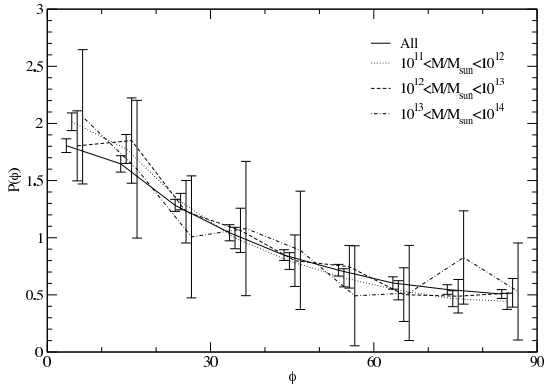
To select the inner parts of each subhalos,  $\zeta_l$  was calculated assuming  $s = 0$ . Particles were then sorted by  $\zeta_l$  and the inner subhalo was selected as a numerical fraction of the subhalo's mass. Once this distribution was defined, the moment of inertia tensor was recalculated, and the eigensystem solved iteratively to determine the inner value of  $s$  (as outlined in Section 3.1).

Fig.2 shows that the inner regions of subhalos appear to be significantly more elliptical than their overall matter distribution. This is in agreement with the findings of others who also reported that dark matter halos tend to increase their asphericity towards the centre (e.g. Jing & Suto 2002; Allgood et al. 2006; Hayashi et al. 2007). We will return to this finding in the following Section when investigating the radial alignment as a function of distance to the centre: Is the signal actually enhanced due to the increase in sphericity? Or does the correlation weaken despite this result?

We would like to note that Allgood et al. (2006) also cautioned that the sphericity may be overestimated if too few particles are used. In order to check the credibility of the trend seen in Fig.2 we recalculated the distributions restricting the haloes to have masses in the range  $M \in [10^{12}, 10^{13}]h^{-1}M_\odot$ . We still observe the same shift in the peak of the distributions; however, the extended tail towards lower  $s$ -values for the inner 10-20% has vanished, i.e. there are hardly any objects with  $s < 0.4$ .

## 3.2 Radial Alignment in 2D

The principal aim of this study is to investigate whether or not there is a dependence of the radial alignment of subhalos (i.e. the alignment of their major axis with respect to the centre of the host) on the mass of their host halo when observing the mass distributions in projection. Recent observational evidence suggests that the major axis (in projection) of satellite galaxies tend to “point towards the centre of their host” (e.g. Pereira & Kuhn 2005; Agustsson & Brainerd 2006; Faltenbacher et al. 2007). It is therefore natural to ask whether or not subhalos in cosmological simulations display a similar trend. To date a few studies have investigated this subject (Knebe et al. 2008; Kuhlen et al. 2007; Faltenbacher et al. 2007; Pereira et al. 2007) all of which used the full 3D spatial information available to them;



**Figure 3.** Correlation of angle between major axes of subhalos and position of the subhalos from the center of their host. We use the same subhalo mass bins as in Fig.1. Error bars (marginally shifted for clarity) are again the square root of the Poisson error and the projection variation.

only Faltenbacher et al. (2007) also presented a 2D analysis. However, a fair comparison to observational findings requires a projection of the simulation data into the observer’s plane.

To measure the radial alignment of our (projected) subhalos, we use the eigenvector  $\mathbf{E}_{a_1}$  which corresponds to the direction of the major axis  $a_1$  of the subhalo. We quantify the radial alignment of subhalos as the angle between the major axis  $\mathbf{E}_{a_1}$  of each subhalo and the radius vector of the subhalo in the reference frame of the host:

$$\cos \phi = \frac{\mathbf{R}_{\text{sub}} \cdot \mathbf{E}_{a_1, \text{sub}}}{|\mathbf{R}_{\text{sub}}| |\mathbf{E}_{a_1, \text{sub}}|}. \quad (4)$$

### 3.2.1 Mass Dependence

In Fig.3 we show the normalized distribution of the angle  $\phi$  as defined via Eq.(4). While the black line shows the signal for all subhalos under consideration, the different lines are representative for various mass bins. We find a positive radial alignment signal different from isotropy, in agreement with other studies (Knebe et al. 2008; Kuhlen et al. 2007; Faltenbacher et al. 2007; Pereira et al. 2007) – even when restricting the analysis to 2D. We further conclude from this plot that no particular mass range is responsible for the signal. We also note that the strength of the signal is substantially stronger than the one seen in observations (cf. Pereira & Kuhn 2005). We will though see in the following Section that this sensitively depends on the point where we measure the actual (projected) shape of the subhalo.

### 3.2.2 Radial Dependence

As with many cosmological  $N$ -body studies, we are considering the orientations of dark matter halos and are comparing them with the distributions of baryons observed in galaxy clusters. Such a comparison can be significantly biased if the observed orientation of galaxies, which occupy the deepest part of the subhalo potential, are not aligned with the global orientation of the dark matter. We examined this effect by studying the dependence of the (projected) radial alignment signal on the point where we measure the subhalos’ shape as outlined in Section 3.1.2.

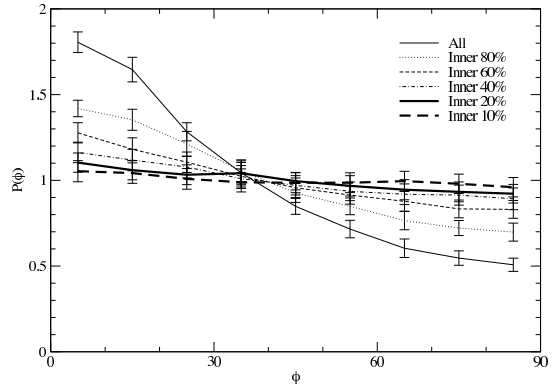


**Figure 4.** Same as Fig.3, but each line shows the correlation using major axes derived from a fraction of particles. The different lines represent shape measures at different mass thresholds. Error bars indicate the projection variation.

The result of selecting the inner particles is quite striking; Fig.4 presents the orientation correlation using different percentage of inner particles in subhalos. We observe a drop in the signal’s strength when restricting to the central parts; considering only the inner 10-20% of particles we recover the observed correlation noted by Pereira & Kuhn (2005): following Struble & Peebles (1985) and Pereira & Kuhn (2005), respectively, we quantify our results in terms of an alignment parameter  $\delta = \sum_i (\phi_i / N) - 45^\circ$ , where  $\phi_i$  are the individual subhalo orientations and  $N$  the number of subhalos. When using all particles in a subhalo we derive a value of  $\delta \approx -11^\circ$ . However, when restricting to the innermost 20% (10%) we obtain  $\delta \approx -2^\circ$  ( $\delta \approx -1^\circ$ ) in agreement with the value reported by Pereira & Kuhn (2005). The weakening of the signal could be due to poorly defined principle axes if the inner distributions of particles were significantly rounder than the overall dark matter distribution. However, we already noted that the distribution of sphericity moves towards smaller values in the inner parts of the subhalos (cf. Fig.2). In that regards caution must also be urged as, for the smallest halos containing of order 100 particles (cf. Section 2.2), considering the inner 10% of particles means that we are measuring principle axes using of order 10 particles, and as such are very sensitive to Poisson noise. In order to avoid such small numbers of particles and to verify the credibility of the weakening of the signal, we repeated the analysis restricting the subhalos to those whose mass is in the range  $10^{12} h^{-1} M_\odot \leq M_{\text{sub}} < 10^{13} h^{-1} M_\odot$ , that is the number of constituent particles is in the range,  $3289 \leq N_p < 32897$ . We recover the same orientation correlation, with the lower the fraction of inner particles, the lower the observed signature of orientation correlation, again bringing into agreement with the observed correlation for the inner 10-20% of particles.

## 4 SUMMARY AND CONCLUSIONS

We have examined whether or not the radial alignment of the major axes of subhalos with respect to the centre of their host dark matter halo is still present when projecting the data from cosmological simulations into the observer’s plane. Our results draw upon a sample of dark matter host

halos spanning group- to cluster-mass scales ( $6 \times 10^{13} h^{-1} M_{\odot}$  to  $6 \times 10^{14} h^{-1} M_{\odot}$ ).

While observations of clusters of galaxies have revealed a mild radial alignment of subhalos with respect to their host (Pereira & Kuhn 2005; Wang et al. 2007) the signal found in our data is substantially stronger. However, when restricting the shape determination to using only the innermost 10-20% of the subhalo's particles we recover the observed correlation strength, in agreement with the results reported by Faltenbacher et al. (2007). We though note that the signal does not weaken because the central parts of subhalos are rounder and hence radial alignment itself becomes ill-defined. On the contrary, in agreement with previous findings we observe the trend for subhalos to become more aspherical when approaching the centre (cf. Jing & Suto 2002; Allgood et al. 2006; Hayashi et al. 2007). Therefore, while the strength of the radial alignment decreases even though the asphericity increases towards the centre there has to be a misalignment between the inner regions of the subhalo and its outer structure. However, it is known that the major axes of the central parts of field halos are aligned with those of the whole object (cf. Jing & Suto 2002). One possible solution to this puzzling observation is tightly coupled to the overall explanation of the radial alignment as a dynamical/tidal effect (Kuhlen et al. 2007; Pereira et al. 2007): it can be surmised that subhalos which have passed through their apocenter must experience a strong tidal field and the outer – more loosely bound – regions of a subhalo will be subject to more distortion than the inner parts. This results in a weaker correlation of the protected inner parts of the sub-halo and the host.

We may even be as bold as to reverse the argumentation and use the (projected) radial alignment to infer the point where the galaxy is expected to lie within the dark matter subhalo: The point where the strength of the signal matches the observed correlation – that is based upon the shape of the galaxy – coincides with 10-20% of the total subhalo mass. Assuming a density profile of the functional form proposed by Navarro et al. (1997, NFW) and a fiducial concentration of about  $c=10-15$  for this profile, 15% of  $M_{\text{vir}}$  is reached at about 9-11% of the virial radius.<sup>3</sup> This is in agreement with the results found by Bailin & Steinmetz (2005) who found that this marks a point where the influence of the baryons becomes important and there appears to be a lack of connection between the inner and outer regions defined by this point, respectively.

## ACKNOWLEDGEMENTS

AK acknowledges funding through the Emmy Noether programme of the DFG (KN 755/1). The simulations were carried out on the super computer of the Center for Computational Astrophysics, the National Astronomical Observatory of Japan (Project-ID: why36b, ihy01b). HY acknowledges the support of the Research Fellowships of the Japan Society for the Promotion of Science for Young Scientists

(17-10511). HY is also thankful to Junichiro Makino and Toshiyuki Fukushige for their useful comments. This research has been undertaken as part of the Commonwealth Cosmology Initiative (<http://www.thecci.org>).

## REFERENCES

- Adelman-McCarthy J. K. e. a., 2007, ApJS, 172, 634  
 Agustsson I., Brainerd T. G., 2006, ApJ, 644, L25  
 Allgood B., Flores R. A., Primack J. R., Kravtsov A. V., Wechsler R. H., Faltenbacher A., Bullock J. S., 2006, MNRAS, 367, 1781  
 Bailin J., Steinmetz M., 2005, ApJ, 627, 647  
 Bett P., Eke V., Frenk C. S., Jenkins A., Helly J., Navarro J., 2007, MNRAS, 376, 215  
 Colless M. e. a., 2003, ArXiv Astrophysics e-prints  
 Davis M., Efstathiou G., Frenk C. S., White S. D. M., 1985, ApJ, 292, 371  
 Dubinski J., Carlberg R. G., 1991, ApJ, 378, 496  
 Faltenbacher A., Jing Y. P., Li C., Mao S., Mo H. J., Pasquali A., van den Bosch F. C., 2007, ArXiv e-prints, 706  
 Faltenbacher A., Li C., Mao S., van den Bosch F. C., Yang X., Jing Y. P., Pasquali A., Mo H. J., 2007, ApJ, 662, L71  
 Freeman K., Bland-Hawthorn J., 2002, ARA&A, 40, 487  
 Frenk C. S., White S. D. M., Davis M., Efstathiou G., 1988, ApJ, 327, 507  
 Hawley D. L., Peebles P. J. E., 1975, AJ, 80, 477  
 Hayashi E., Navarro J. F., Springel V., 2007, MNRAS, 377, 50  
 Jing Y. P., Suto Y., 2002, ApJ, 574, 538  
 Kase H., Makino J., Funato Y., 2007, PASJ, 59, 1071  
 Kasun S. F., Evrard A. E., 2005, ApJ, 629, 781  
 Katz N., 1991, ApJ, 368, 325  
 Kazantzidis S., Mayer L., Mastropietro C., Diemand J., Stadel J., Moore B., 2004, ApJ, 608, 663  
 Klypin A., Gottlöber S., Kravtsov A. V., Khokhlov A. M., 1999, ApJ, 516, 530  
 Knebe A., Draganova N., Power C., Yepes G., Hoffman Y., Gottloeber S., Gibson B. K., 2008, ArXiv e-prints, 802  
 Knebe A., Green A., Binney J., 2001, MNRAS, 325, 845  
 Kravtsov A. V., Berlind A. A., Wechsler R. H., Klypin A. A., Gottlöber S., Allgood B., Primack J. R., 2004, ApJ, 609, 35  
 Kravtsov A. V., Klypin A. A., Khokhlov A. M., 1997, ApJS, 111, 73  
 Kuhlen M., Diemand J., Madau P., 2007, ApJ, 671, 1135  
 Macciò A. V., Dutton A. A., van den Bosch F. C., Moore B., Potter D., Stadel J., 2007, MNRAS, 378, 55  
 Makino J., Fukushige T., Koga M., Namura K., 2003, PASJ, 55, 1163  
 Nagashima M., Yahagi H., Enoki M., Yoshii Y., Gouda N., 2005, ApJ, 634, 26  
 Navarro J. F., Frenk C. S., White S. D. M., 1997, ApJ, 490, 493  
 Pereira M. J., Bryan G. L., Gill S. P. D., 2007, ArXiv e-prints, 707  
 Pereira M. J., Kuhn J. R., 2005, ApJ, 627, L21  
 Pfitzer D., Salmon J., Sterling T., 1997, CACR Technical Reports, 150, 0  
 Spergel et al. D. N., 2003, ApJS, 148, 175

<sup>3</sup> Even though tidal stripping will affect the outer regions of subhalos the central parts will still follow a (simple) power-law density profile as given by, for instance, the NFW profile (cf. Kazantzidis et al. 2004).

- Spergel et al. D. N., 2007, ApJS, 170, 377  
Struble M. F., Peebles P. J. E., 1985, AJ, 90, 582  
Teyssier R., 2002, A&A, 385, 337  
Thompson L. A., 1976, ApJ, 209, 22  
Wang Y., Yang X., Mo H. J., Li C., van den Bosch F. C.,  
Fan Z., Chen X., 2007, ArXiv e-prints, 710  
Warren M. S., Quinn P. J., Salmon J. K., Zurek W. H.,  
1992, ApJ, 399, 405  
Yahagi H., 2005, PASJ, 57, 779  
Yahagi H., Yoshii Y., 2001, ApJ, 558, 463

This paper has been typeset from a  $\text{\TeX}/\text{\LaTeX}$  file prepared  
by the author.